Estimation of relative position and coordination of mobile underwater robotic platforms through electric sensing.

Yannick Morel, Mathieu Porez, Auke Ijspeert

Estimation of Relative Position and Coordination of Mobile Underwater Robotic Platforms through Electric Sensing

Yannick Morel, Mathieu Porez, and Auke J. Ijspeert

***Abstract*— In the context of underwater robotics, positioning and coordination of mobile agents can prove a challenging problem. To address this issue, we propose the use of electric sensing, with a technique inspired by weakly electric fishes. In particular, the approach relies on one or several of the agents applying an electric field to their environment. Using electric measures, others agents are able to reconstruct their relative position with respect to the emitter, over a range that is function of the geometry of the emitting agent and of the power applied to the environment. Efficacy of the technique is illustrated using a number of numerical examples. The approach is shown to allow coordination of unmanned underwater vehicles, including that of bio-inspired swimming robotic platforms.**

I. Introduction

Underwater robotic technology has undergone over the past few decades a radical transformation, driven to a large extent by advances in unmanned systems' autonomy. This improved autonomy has brought about a paradigm shift in the use of underwater robotic systems, from tethered, remotely operated vehicles, towards untethered, autonomous solutions capable of operating with little supervision over extended periods of time. The transition opened the door to a number of previously inaccessible scenarii, such as large scale oceanographic surveys ([1–3]), or extended-horizon area surveillance ([4]). Yet, there remains a number of challenges, particular to the underwater environment, which constitute significant hurdles in the way of greater achievements.

Prominent among these is the problem of underwater positioning for mobile systems, and in particular that of relative positioning for groups of cooperating underwater agents. More specifically, unmanned underwater systems, while submerged, are unable to directly access information relayed by the Global Positioning System (GPS) constellation. Instead, underwater vehicles have come to rely on a number of alternate solutions, including inertial navigation and acoustic positioning systems ([5]). In the following, we propose a novel method for positioning and coordination of robotic underwater platforms, based on electrical sensing. Application of an electric sense to underwater robotics has in the past been considered, in particular to allow detection of obstacles ([6–10]). However, to the best of our knowledge, use of such an electric sense to address the relative positioning problem for mobile underwater robotic platforms had yet to be investigated. The approach relies on the platforms being equipped with a set of electrodes, which they may use to either apply an electric field to their environment, or measure electric variables, such as electric potential differences or electric currents. Having one or several mobile agents applying an electric field to their environment allows other agents in the group to infer some measure of information regarding their surroundings, and in particular to estimate relative positions. The approach's strengths and weaknesses are in direct contrast to that of aforementioned positioning technologies. In particular, the proposed positioning scheme is only effective at close ranges (up to a few meters). However, it is well suited to unknown, unstructured, and cluttered environments.

Note that the electric sense's greatest strength, however, lies in its aptitude to detect conductive objects underwater with ease. As a result, a mobile marine platform equipped with such a sense is capable of detecting metallic objects and structures, such as underwater cables, pipelines and wrecks. However, detection only occurs at short range. Hence, if a single platform will (eventually) be successful in searching a given area for metallic objects, mission success may require time. To mitigate the issue, one may use a group of such mobile platforms, pursuing the assigned detection task in a collaborative manner. In particular, using the relative positioning scheme described hereafter, it becomes possible to coordinate motion of a group of electric sensing agents, so as to ensure juxtaposition of sensing areas. As a result, the group is able to scan for metallic objects over an area proportional to the number of agents in the group.

The positioning algorithm described in the following is designed to be simple and practical. In particular, the method relies on an approximate model of the effect of relative position between an emitting agent (agent emitting an electric field) and a passive agent (measuring electric potential differences or currents) on the electric measures made by the latter. This model is constructed from input/output data, using a polynomial neural network ([11], [12]). Weierstrass' theorem ([13]) shows that it is possible to construct this model in such a manner that it approximates the actual relationship with arbitrary accuracy. Then, to estimate the relative position corresponding to a given set of electric measures, one may present this model with a set of candidate relative positions. We will show that, for a sufficient number of measures, it

This work was supported by the European Commission, Information Society and Media, Future and Emerging Technologies (FET), ANGELS project, contract number: 231845.

Y. Morel is with the BioRobotics Laboratory, Bioengineering Institute, Ecole Polytechnique Fédérale de Lausanne (EPFL), CH-1015 Lausanne, Switzerland, yannick.morel@epfl.ch

M. Porez is with the IRCCyN Laboratory, Mines de Nantes, 44307 Nantes, France, mathieu.porez@mines-nantes.fr

A. J. Ijspeert is with the Faculty of Bioengineering (BioRobotics Laboratory), Ecole Polytechnique Fédérale de Lausanne (EPFL), CH-1015 Lausanne, Switzerland, auke.ijspeert@epfl.ch

Preprint submitted to 2012 IEEE International Conference on Robotics and Automation. Received September 16, 2011.

is possible to identify likelier candidate relative positions by comparing the corresponding model's output to the actual measures.

This paper is structured as follows. Section II describes the proposed algorithm, which allows reconstruction of the relative position between passive and active agents using electric measures. The technique is applied to a specific agent geometry in Section III. Results of numerical simulations are provided in Section IV and illustrate efficacy of the approach. Section V concludes this paper.

II. Estimation of Relative Positions through Electric Sensing

Consider a mobile robotic platform, immersed in a conductive environment. Assume it is able to apply an electric field to its environment. Spatial features of the resulting field are a direct consequence of the emitter's geometry, attitude and position. Hence, when applying an electric field to its environment, the emitter is injecting information regarding its situation in this environment. In the following, we develop a technique allowing to leverage this information to estimate the relative position of mobile underwater platforms. In theory, the issue could be addressed using analytical means, for instance using a closed form model of the electric field as generated by the emitter, and analyzing model invertibility. However, derivation of one such model might prove difficult, and, depending on the level of accuracy required, the resulting closed form might prove unwieldy. Rather, construction of the proposed positioning technique relies on a numerical simulation of the generated field, based on the Boundary Elements Method (BEM, [14], [15]). A detailed presentation of the simulation tool used is beyond the scope of this paper, but the interested reader is referred to [16]. Note that this numerical tool is only used in the development of the proposed algorithm. Ultimately, the latter is self-contained and does not require presence of the former to operate.

In the following, we discuss the possibility of constructing an approximate closed-form model, using polynomial neural networks to emulate the relationship from relative positions to electric measures, as well as the manner in which we may exploit this neural model to estimate relative positions.

A. From Relative Position to Currents

Consider two robotic platforms featuring a set of electrodes. One of these platforms is using its electrodes to apply an electric field to its environment (active platform), while the second is measuring electrode currents, using configurations similar to that described in Figure 1. For fixed platforms' geometry, there exists an algebraic, continuous relationship between the position and attitude of the emitter with respect to the receiver, and the value of electric measures performed by the receiver.

For ease of exposition, we limit discussions to a two-dimensional case. In addition, let the attitude of the active and passive agents be described by $\psi_1(t)$, $\psi_2(t) \in (-\pi, \pi]$, $t \geqslant 0$, respectively. Let the platforms' relative attitude be noted $\psi_{\mathrm{r}}(t) \triangleq \psi_1(t) - \psi_2(t)(2\pi)$, $\psi_{\mathrm{r}}(t) \in (-\pi, \pi]$, and

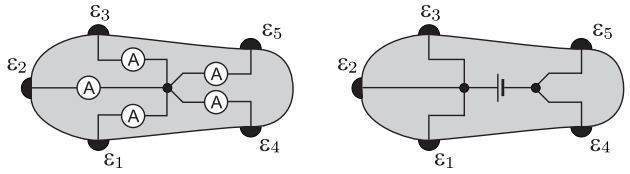

Fig. 1. Schematic view of the electric configuration of passive (left) and active (right) platforms, where ε_j, $j = 1, \ldots, 5$, represent electrodes mounted on the platform's surface, in contact with a conductive environment (represented platform shape is arbitrary).

their relative position be characterized by relative bearing $\rho(t) \in (-\pi, \pi]$ and distance $d(t) \geqslant 0$. Furthermore, let $i_{\mathrm{v}}(t) \in \mathbb{R}^n$ be the vector of n electrode currents measured by the passive platform (e.g. the currents measured between electrodes ε_j, $j = 1, \ldots, 5$, and the central connecting point in Figure 1, left). Numerical simulations and experimental measures show that the following function,

$$\begin{array}{rccl} f: & (-\pi, \pi] \times (-\pi, \pi] \times \mathbb{R}^{+*} & \rightarrow & \mathcal{D}_i, \\ & \psi_{\mathrm{r}},\, \rho,\, d & \rightarrow & i_{\mathrm{v}}, \end{array} \tag{1}$$

where $\mathcal{D}_i \subseteq \mathbb{R}^n$ represents the range of $f(\psi_{\mathrm{r}}, \rho, d)$ for $(\psi_{\mathrm{r}}, \rho, d) \in (-\pi, \pi] \times (-\pi, \pi] \times \mathbb{R}^{+*}$, is a well behaved, continuous function of its arguments (see Figure 3 to Figure 5). Ideally, we would like to access the inverse relationship $f^{-1}(i_{\mathrm{v}})$; that is, obtain ψ_{r}, ρ and d from the measured i_{v}. However, it is not certain that $f(\cdot)$ even is one-to-one onto. Clearly, that is unlikely to be the case for a low number of measures, but possible for greater numbers. Formally addressing the issue of invertibility would require an analytical expression of the relationship, which is not available to us. Instead, rather than a theoretical proof of invertibility, the following will provide a proof by example. In particular, we show that for a sufficient number of electrodes, we are indeed able to estimate relative bearing $\rho(t)$, $t \geqslant 0$, and distance $d(t) \geqslant 0$, within a given range.

B. Neural-based Functional Approximation

We begin by designing an approximate relationship $\hat{f}(\cdot)$, intended to emulate the input/output map of $f(\cdot)$. To facilitate proceedings, define $x \triangleq \left[\begin{array}{ccc} \psi_{\mathrm{r}} & \rho & d \end{array} \right]^{\mathrm{T}}$, and $\mathcal{D}_x \triangleq (-\pi, \pi] \times (-\pi, \pi] \times \mathbb{R}^{+*}$. The relationship $f(x)$ being a continuous function of its arguments over $\mathcal{D}_x$, we conclude from Weierstrass' approximation theorem ([13]) that for any given $\epsilon_x > 0$, there exists a polynomial function $\hat{f}(x)$ on $\mathcal{D}_x$ such that

$$\| f(x) - \hat{f}(x) \| < \epsilon_x, \quad x \in \mathcal{D}_x. \tag{2}$$

A classical manner in which one may construct $\hat{f}(x)$ is by adopting a neural network formalism ([17]). In particular, let

$$\hat{f}(x) \triangleq W \sigma(x), \quad x \in \mathcal{D}_x, \tag{3}$$

where $W \in \mathbb{R}^{n \times p}$ is a weight matrix, and $\sigma(x) \in \mathbb{R}^p$ a nonlinear function of its argument. To select appropriate W and $\sigma(\cdot)$, it is necessary to have access to input/output data characterizing the function to be approximated, $f(x)$. In particular, assume that, for a number of inputs x_j, $j = 1, \ldots, q$, we have access to the corresponding $f(x_j)$. Then,

$$W^* \triangleq \left[\begin{array}{ccc} f(x_1) & \ldots & f(x_q) \end{array} \right] \left[\begin{array}{ccc} \sigma(x_1) & \ldots & \sigma(x_q) \end{array} \right]^{\dagger}, \tag{4}$$

Preprint submitted to 2012 IEEE International Conference on Robotics and Automation. Received September 16, 2011.

where $\cdot^\dagger$ denotes the Moore-Penrose pseudo-inverse, minimizes in the least-mean-squared sense the approximation error $f(x_j) - \hat{f}(x_j)$, $j = 1, \ldots, q$. Using (4) to select W in (3) for a particular $\sigma(x)$, for sufficiently smooth functions $f(x)$, it is oftentimes possible to iteratively select the vector $\sigma(\cdot)$ to reach a desired accuracy ϵ_x.

C. Inverting the Relationship

To exploit the approximate model in constructing a position estimate, we define the following current error,

$$e_i(i_\mathrm{v}(t), x_\mathrm{c}) \triangleq \|i_\mathrm{v}(t) - \hat{f}(x_\mathrm{c})\|, \quad t \geqslant 0, \tag{5}$$

where x_c represents a candidate, possible relative position. We select the relative position estimate as follows,

$$\hat{x}(t) \triangleq \underset{x_\mathrm{c} \in \mathcal{D}_x}{\triangleq \operatorname{argmin}} e_i(i_\mathrm{v}(t), x_\mathrm{c}), \quad t \geqslant 0. \tag{6}$$

This choice is motivated by the following proposition.

Proposition 2.1: Consider a relationship $f : \mathcal{D}_x \to \mathcal{D}_i \subseteq \mathbb{R}^n$, assumed to have a continuously differentiable inverse over $\mathcal{D}_i$. In addition, assume there exists an approximation of $f(x)$, noted $\hat{f}(x)$, and let $\epsilon(x)$ denote the approximation error, such that

$$\hat{f}(x) = f(x) + \epsilon(x), \quad x \in \mathcal{D}_x. \tag{7}$$

Finally, assume one is able to find an estimate $\hat{x}$ of the actual x, such that

$$\hat{f}(\hat{x}) = f(x) + \epsilon_i, \tag{8}$$

where $\epsilon_i \in \mathbb{R}^n$. Then, the norm of $x - \hat{x}$ is upper-bounded by a Positive Definite (PD) function of ϵ_i, $\epsilon(\hat{x})$.

Proof: As $f^{-1} : \mathcal{D}_i \to \mathcal{D}_x$ is continuously differentiable over $\mathcal{D}_i$, it is globally Lipschitz over $\mathcal{D}_i$. Hence, there exists $l \in \mathbb{R}^{+*}$ such that

$$\|f^{-1}(f(x)) - f^{-1}(f(\hat{x}))\| \leqslant l\|f(x) - f(\hat{x})\|. \tag{9}$$

Simplifying the left-hand side of (9) and substituting (7) and (8) into (9), we obtain

$$\begin{aligned} \|x - \hat{x}\| &\leqslant l\|f(x) - (\hat{f}(\hat{x}) - \epsilon(\hat{x}))\| \\ &\leqslant l\|f(x) - f(x) - \epsilon_i + \epsilon(\hat{x})\| \\ &\leqslant l(\|\epsilon_i\| + \|\epsilon(\hat{x})\|), \end{aligned} \tag{10}$$

where the right-hand-side is a PD function of ϵ_i, $\epsilon(\hat{x})$. ■

Significance of the above is that, assuming the inverse function is sufficiently smooth, the better our functional approximation and the closer we match the measured current, the more accurate the position estimate.

D. Measure of Relative Heading

In practice, one may use an electronic compass to measure attitude. Hence, assuming the agents are able to communicate, the relative heading $\psi_\mathrm{r}(t)$ does not need to be reconstructed. Therefore, we need not entirely invert $f(\cdot)$. In particular, when looking for candidate relative positions $x_\mathrm{c} = \begin{bmatrix} \psi_\mathrm{rc} & \rho_\mathrm{c} & d_\mathrm{c} \end{bmatrix}^\mathrm{T}$ to minimize (5), we do not need to consider selection of ψ_rc. Rather, we may use $x_\mathrm{c} = \begin{bmatrix} \psi_\mathrm{r} & \rho_\mathrm{c} & d_\mathrm{c} \end{bmatrix}^\mathrm{T}$, and focus on selecting the relative bearing $\hat{\rho}$ and distance $\hat{d}$ which minimize (5). In summary, the proposed positioning algorithm consists in, given an approximate relationship $\hat{f}(\cdot)$, current measure i_v, and relative heading ψ_r, selecting estimated relative bearing $\hat{\rho}$ and distance $\hat{d}$ which minimize the current matching error (5).

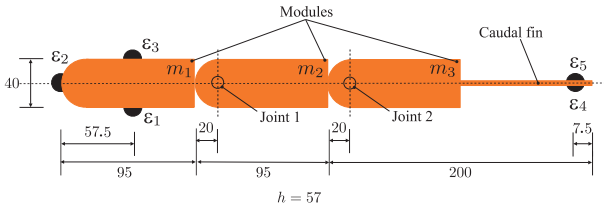

Fig. 2. Swimming robot AmphiBotIII, in a three-module configuration, equipped with a set of five electrodes ε_j, $j = 1, \ldots, 5$ (lengths in mm).

III. Application to AmphiBotIII

In this section, we apply the relative positioning algorithm described in Section II to the case of an actual mobile marine robotic platform, AmphiBotIII ([18]). AmphiBot is a modular robot, constituted of a number of identical modules, linked together with actuated revolute joints. The platform's geometry is described in Figure 2. The robot is constituted of three modules and a caudal fin. We assume it is equipped with a set of five electrodes, as shown in Figure 2. We consider a pair of such platforms, one of them being active, with a difference of potential between the group of electrodes 1 to 3 (head electrodes) and electrodes 4 and 5 (tail electrodes) of 10V, and the second in a passive configuration, in which currents are measured as described in Figure 1 (left). In the following, we construct $\hat{f}(\cdot)$ in successive steps. In particular, we begin by addressing the influence of relative heading ψ_r on the measured currents in i_v, then that of distance d, and finally of relative bearing ρ.

A. Effect of Relative Heading on Current Measures

To understand how to design $\sigma(\cdot)$ in (3), we assign particular relative positions to our platforms, and evaluate the manner in which the relative position affects measured currents. Relative position is here defined as the position from the rotation axis of joint 2 (see Figure 2) of the passive agent, to that of the active agent. Furthermore, we for now assume that the platforms remain in a straight geometrical configuration, as shown in Figure 2. The platform's attitude is characterized by the angle between its longitudinal axis and a given, geographically fixed direction.

We place our platforms at fixed relative distance and bearing ($d = 1.0625$m, $\rho = 32.4$deg), and vary ψ_r from 0 to 2πrad. We obtain the current measures shown in Figure 3 in solid. To capture the influence of ψ_r on i_v, we use

$$\sigma_1(\psi_\mathrm{r}) = \begin{bmatrix} 1 & \psi_\mathrm{r} & \ldots & \psi_\mathrm{r}^{p_1-1} \end{bmatrix}^\mathrm{T} \in \mathbb{R}^{p_1}, \quad \psi_\mathrm{r} \in (-\pi, \pi], \tag{11}$$

where $p_1 \in \mathbb{N}^*$. To construct a weight matrix W_1 such that $W_1\sigma_1(\psi_\mathrm{r})$ offers a convincing rendition of $i_\mathrm{v}(\psi_\mathrm{r})$, we use (4), with values of ψ_r spanning $(-\pi, \pi]$ with a given step δ_ψ. For illustration, we constructed $W_1\sigma_1(\psi_\mathrm{r})$ with $p_1 =$

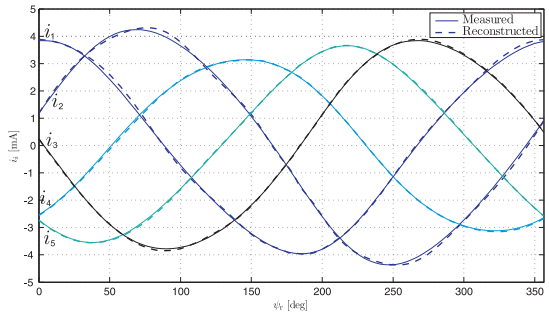

Fig. 3. Measured currents for all five electrodes, for a distance $d = 1.0625$m, at relative angle $\rho = 32.4$deg, with $p_1 = 16$.

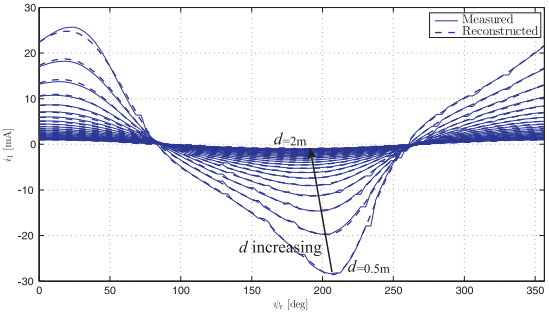

Fig. 4. Measured currents i_1, for distances from $d = 0.5$m to 2m, at relative angle $\rho = 32.4$deg, with $p_1 = 16$, $p_2 = 8$.

16, $\delta_\psi = 3.6$deg. The approximation is shown in Figure 3 (dashed), and is in good agreement with actual values.

B. Effect of Relative Distance on Current Measures

Amplitude of i_v decreases with d, as shown in Figure 4, which presents i_1 (measure corresponding to electrode ε_1), for $\psi_r \in (-\pi, \pi]$, and d varying from 0.5m to 2m with a step $\delta_d = 0.0625$m. To account for the influence of d on i_v, we construct a new σ–vector,

$$\sigma_2(\psi_r, d) = \begin{bmatrix} I_{p_2} & \psi_r I_{p_2} & \dots & \psi_r^{p_1-1} I_{p_2} \end{bmatrix}^T \begin{bmatrix} 1 & d & \dots & d^{p_2-1} \end{bmatrix}^T,$$
$$\sigma_2(\psi_r, d) \in \mathbb{R}^{p_1 p_2}, \quad \psi_r \in (-\pi, \pi], \quad d \in [0.5, 2], \quad (12)$$

where $I_m \in \mathbb{R}^{m \times m}$ denotes the $m \times m$ identity matrix. We repeat the same procedure as above to obtain W_2 so that $W_2 \sigma_2(\psi_r, d)$ approximates $i_v(\psi_r, d)$ over $\psi_r \in (-\pi, \pi]$, $d \in [0.5, 2]$, with $p_1 = 16$, $p_2 = 8$, $\delta_\psi = 3.6$deg, and a distance step $\delta_d = 0.0625$m. Approximation results are shown in Figure 4 in dashed. The reconstructed current is in good agreement with the measured values.

C. Effect of Relative Bearing on Current Measures

Finally, we consider a case in which we fix $d = 1.0625$m, $\psi_r = 68.4$deg, and vary ρ from 0 to 2πrad. The corresponding current measures are shown in Figure 5. As the σ–vector is becoming large, we avoid further extending $\sigma_2(\cdot)$, but instead adjust the weight matrix to be function of ρ. In particular, we repeat the process described in the previous section for different values of relative bearing. More specifically, we repeat this process for $\rho \in (-\pi, \pi]$, with steps $\delta_\rho = 3.6$deg. Visualizing the values of the weight matrix for different values of ρ is unfortunately not helpful, as clear trends are difficult to recognize. Hence, rather than

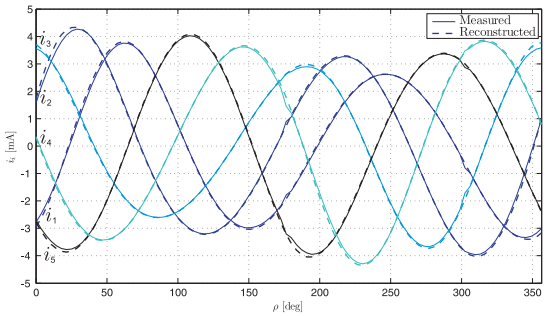

Fig. 5. Measured currents for all five electrodes, for a distance $d = 1.0625$m, at relative direction $\psi_r = 68.4$deg, with $p_1 = 16$, $p_2 = 8$.

parameterizing the weight matrix as a function of ρ, we use linear interpolation between computed cases to estimate the appropriate weight matrix for a given relative bearing. Achieved results are convincing, as illustrated by Figure 5, where reconstructed currents are dashed. In summary, our approximate model is of the form

$$\hat{f}(\psi_r, \rho, d) = W(\rho)\sigma(\psi_r, d), \quad (\psi_r, \rho, d) \in \mathcal{D}_x, \quad (13)$$

where for a given ρ, $W(\rho)$ is linearly interpolated between weight values computed for different relative bearings, and $\sigma(\psi_r, d) \equiv \sigma_2(\psi_r, d)$, $\psi_r \in (-\pi, \pi]$, $d \in [0.5, 2]$.

D. Numerical Application

In the following, we use the approximate model given by (13) to estimate the relative position in a particular case. We chose one such arbitrary relative position, located within $\mathcal{D}_x$. In particular, we select $\psi_r = 58$deg, $\rho = 300$deg, and $d = 0.8$m. We obtain the current measure $i_v = \begin{bmatrix} -1.3443 & -7.5840 & -3.4427 & 5.2550 & 7.1160 \end{bmatrix}^T$mA.

To estimate the relative position, we construct the surface $e_i(i_v, \psi_r, \rho_c, d_c)$ for values of $(\rho_c, d_c) \in (-\pi, \pi] \times [0.5, 2]$. This surface is shown in Figure 6, where the actual relative position is marked with a red, dashed line, and the estimate (located at the surface minimum) with a green dot. The estimated values are $\hat{\rho} = 298.8$deg and $\hat{d} = 0.8125$m (for actual values $\rho = 300$deg and $d = 0.8$). Note that, in the construction of $\hat{f}(\cdot)$ and minimization of (5), a great variety of techniques may be used. It is not claimed that the methods used here are optimal in nature, but rather that the solutions proposed are functional, as illustrated by the examples presented in the following section.

IV. Illustrative Numerical Examples

This section presents examples illustrating efficacy of the proposed technique. We consider the motion of AmphiBotIII robotic platforms ([16], [18]). Examples are presented in order of increasing complexity, and treat both rigid and deforming (swimming) agents. In the second example, the estimate is used to enforce a desired relative position, thereby showing electrical sensing-based coordination between swimming robotic platforms.

Preprint submitted to 2012 IEEE International Conference on Robotics and Automation. Received September 16, 2011.

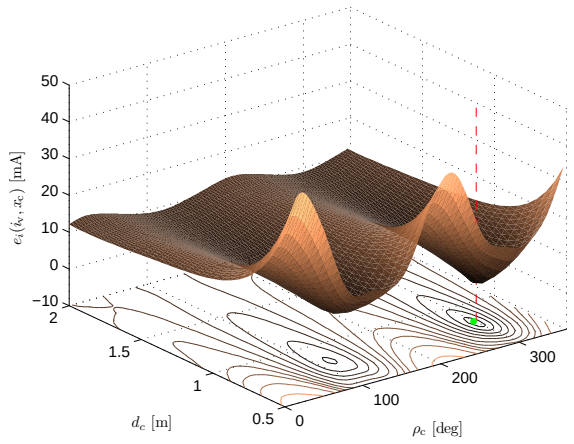

Fig. 6. Current error $e_i(\rho_c, d_c)$ in mA, as a function of candidate distance d_c and direction ρ_c, with $p_1 = 12$, $p_2 = 5$.

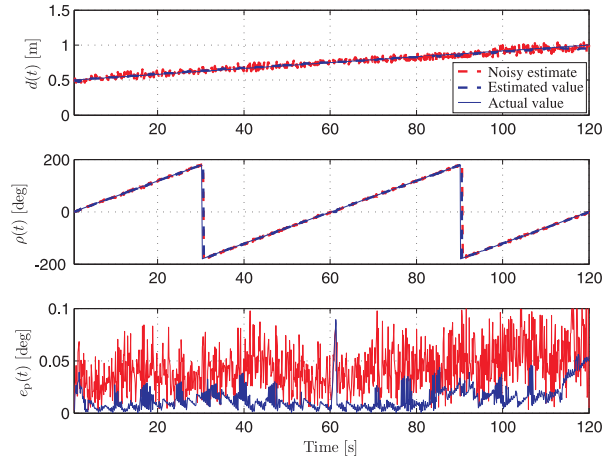

Fig. 7. Rigid Platform case, relative bearing and distance estimation (top and middle), position error (bottom).

A. Rigid Platforms

In this first example, the passive agent is located at the origin, while the active agent is made to circle the origin. We set $\psi_r(t) = (\pi/6)\cos(4\pi/15t)$rad, $\rho(t) = 2\pi t/60$rad, and $d(t) = (1/2)(1 + t/120)$m, $t \in [0, 120]$. The approximate model $\hat{f}(\cdot)$ was developed as described in the previous section, with $p_1 = 12$, $p_2 = 5$.

At initial time, we used a three step iterative position estimation procedure, with $\rho_c \in (-\pi, \pi]$, $d_c \in [0.5, 2]$, $\delta_\rho = 32.73$deg, and $\delta_d = 0.17$m; a second step with a candidate grid centered on the previous step's likeliest candidate position, of dimensions 45deg in ρ, 0.4m in d, with $\delta_\rho = 4.09$deg, and $\delta_d = 4.44$cm; and a final step with grid dimensions of 20deg in ρ, 0.1m in d, with $\delta_\rho = 1.82$deg, $\delta_d = 1.11$cm. For all successive times, at a frequency of 50Hz, we use a similar three step iterative procedure, whose first grid is centered on the position estimate obtained at the previous time instant. The first step's grid dimensions are 80deg in ρ ($\delta_\rho = 7.27$deg) and 1.5m in d ($\delta_d = 16.7$cm); the second step uses 20deg in ρ ($\delta_\rho = 1.82$deg) and 0.4m in d ($\delta_d = 4.4$cm); the final step uses 10deg in ρ ($\delta_\rho = 0.91$deg) and 0.1m in d ($\delta_d = 1.1$cm).

Results are shown in Figure 7, which presents actual and estimated positions (solid and dashed blue, respectively). To evaluate the effect of current measure noise, we applied a zero-mean, additive flat random noise to the value of i_v provided to the algorithm. The noise was scaled so that its magnitude corresponds to 20% of $\|i_v(t)\|$. Position estimates obtained using noisy measures are shown in red, dashed. The algorithm is successful in reconstructing relative distance and bearing (see Figure 7). Norm of the estimation error can be computed as $e_p(t) \triangleq \sqrt{d^2(t) + \hat{d}^2(t) - 2d(t)\hat{d}(t)\cos(\rho(t) - \hat{\rho}(t))}$. This error is shown in Figure 7 (bottom). The value obtained without noise is shown in blue. Mean error is 1.51cm, with standard deviation 4.03cm. The average distance over the simulation being 0.75m, the mean error corresponds to 2% of the average range. The position error obtained with noise is shown in red, with a mean of 4.46cm (6% of the average range), and standard deviation 4.34cm.

B. Deforming Platforms

In a second example, we couple the proposed estimation algorithm with motion control of swimming agents, using the multi-physics simulation detailed in [16]. We consider a first, active agent traveling in a straight line (in the direction $\psi = \pi/6$rad). The passive agent uses the proposed algorithm to estimate its relative position with respect to the other. In addition, we specify desired distance and bearing for the passive agent ($d_d = 0.75$m and $\rho_d = 90$deg, respectively) and close the loop using the control algorithm in [19]. Motion is created using the following Central Pattern Generator (CPG, [18]) parameters; an oscillation amplitude $A = 30$deg, frequency $\nu = 0.85$Hz, and number of waves $K = 0.275$.

Results of relative position estimation are shown in Figure 8. While the estimation still performs well, we notice a slight performance decrease over the rigid case. In particular, the mean position error is 8.19cm without noise (11% of steady state range), with standard deviation 16.93cm. The mean position error reaches 9.08cm (12% of the range), with standard deviation 18.12cm, when including the same zero-mean random measurement noise as considered in the previous example. However, while position estimation could be improved, we are effective in enforcing a specific relative position between swimming agents, as the relative distance and bearing converge to (a neighborhood of) their desired values, as seen in Figure 8 (top and middle, desired value shown in green). Figure 9 shows the trajectory of the swimmers. The passive agent's desired position is shown in red, while its actual relative position is shown in black. As seen in Figure 9, after a short transient, the passive agent's position oscillates about the desired position.

V. Conclusion

This paper presents a relative position estimation technique for mobile underwater robotic platforms. The approach relies on electric sensing. More specifically, an approximation of the relationship from relative position to performed current

Preprint submitted to 2012 IEEE International Conference on Robotics and Automation. Received September 16, 2011.

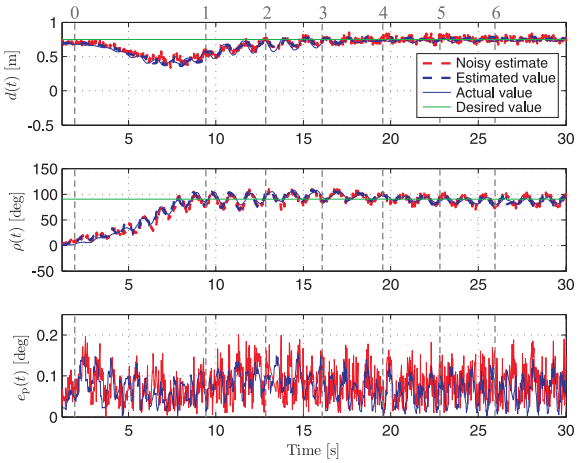

Fig. 8. Swimming case, relative bearing and distance estimation (top and middle), position error (bottom).

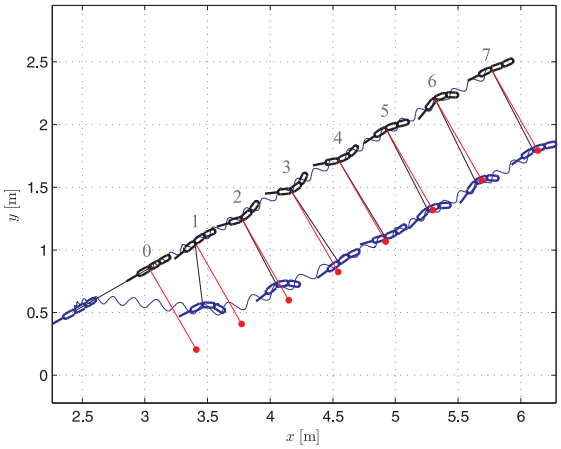

Fig. 9. Swimming case, movement of the platforms.

measures is constructed using polynomial neural networks. Then, this approximate model is used, for given measured currents and relative heading, to reconstruct the relative position of an agent with respect to an electrically active platform. The approach was shown to perform well for both rigid and deforming (swimming) platforms, and allows to coordinate motion of swimming robots. To the best of our knowledge, the presented algorithm is the first to use electric sensing to reconstruct relative positions of mobile agents. Use of this electric sense to allow coordination of swimming agents is also novel. Extension of the proposed technique to include cases featuring a greater number of agents and/or obstacles is currently investigated. Preliminary results are promising and show that, while the presence of additional agents (or obstacles) in-between agents attempting to reconstruct their relative positions does lead to a distortion of the estimate, the issue is easily circumvented by coordinating the group's electric activity (e.g. using a token-based coordination scheme). Another aspect being currently investigated is the extension from a 2-Dimensional (2D) case to 3D. The BEM model used in the work presented here can be scaled to provide a good approximation of the 3D case, and preliminary results show the proposed approach generalizes well to 3D. Finally, implementation of the algorithm on actual robotic platforms, including Electro-Amphibot ([18]), and the ANGELS platform ([20]), is currently underway.

References

[1] D. Crimmins, C. Deacutis, E. Hinchey, M. Chintalaand, G. Cicchetti, and D. Blidberg, "Use of a long endurance solar powered autonomous underwater vehicle (SAUV II) to measure dissolved oxygen concentrations in Greenwich Bay, Rhode Island, U.S.A," in *Proc. 2005 IEEE Oceans - Europe*, vol. 2, (Brest, France), pp. 896–901, 2005.

[2] E. Fiorelli, N. E. Leonard, P. Bhatta, D. A. Paley, R. Bachmayer, and D. M. Fratantoni, "Multi-AUV control and adaptive sampling in Monterey Bay," *IEEE Journal of Oceanic Engineering*, vol. 31, no. 4, pp. 935–948, 2006.

[3] J. Das, K. Rajany, S. Frolovy, F. Pyy, J. Ryany, D. A. Caron, and G. S. Sukhatme, "Towards marine bloom trajectory prediction for AUV mission planning," in *Proc. 2010 IEEE Int. Conf. on Robotics and Automation*, (Anchorage, AK), 2010.

[4] M. C. Stuwart and J. Pavlos, "A means to networked persistent undersea surveillance," in *Proc. 2006 Submarine Technology Symposium*, (Laurel, MD), 2006.

[5] J. J. Leonard, A. A. Bennett, C. M. smith, and H. J. S. Feder, "Autonomous underwater vehicle navigation," *MIT Marine Laboratory Technical Memorandum 98-1*, 1998.

[6] G. Baffet, F. Boyer, and P. B. Gossiaux, "Biomimetic localization using the electrolocation sense of the electric fish," in *Proc. 2008 IEEE Int. Conf. on Robotics and Biomimetics*, (Bangkok, Thailand), 2008.

[7] J. R. Solberg, K. M. Lynch, and M. A. McIver, "Active electrolocation for underwater target localization," *The International Journal on Robotic Research*, vol. 27, no. 5, pp. 529–548, 2008.

[8] M. Alamir, O. Omar, N. Servagent, A. Girin, P. Bellemain, V. LeBastard, P. B. Gaussiaux, F. Boyer, and S. Bouvier, "On solving inverse problems for electric fish like robots," in *Proc. 2010 IEEE Int. Conf. on Robotics and Biomimetics*, (Tianjin, China), 2010.

[9] V. LeBastard, C. Chevallerau, A. Amrouche, B. Jawad, A. Girin, F. Boyer, and P. B. Gossiaux, "Underwater robot navigation around a sphere using electrolocation sense and kalman filter," in *Proc. 2010 IEEE/DSJ Int. Conf. on Intelligent Robots and Systems*, (Taipei, Taiwan), 2010.

[10] M. Sim and D. Kim, "Electrolocation with an electric organ discharge waveform for biomimetic application," *Adaptive Behavior*, vol. 19, no. 3, pp. 172–186, 2011.

[11] Y. Shin and J. Ghosh, "Approximation of multivariate functions using ridge polynomial networks," in *Proc. IEEE Int. Joint Conf. on Neural Networks 1992*, vol. 2, (Baltimore, MD), pp. 380–385, 1992.

[12] C. K. Chak, G. Feng, and C. M. Cheng, "Orthogonal polynomials neural network for function approximation and system modeling," in *Proc. IEEE Int. Joint Conf. on Neural Networks 1992*, vol. 1, (Beijing, China), pp. 594–599, 1995.

[13] H. Jeffreys and B. S. Jeffreys, *Methods of Mathematical Physics,* 3rd Ed. Cambridge, England: Cambridge University Press, 2000.

[14] P. K. Banerjee, *The Boundary Element Methods in Engineering*. McGraw-Hill College, 1994.

[15] Y. Liu, *Fast Multiple Boundary Element Method*. Cambridge, UK: Cambridge University Press, 2009.

[16] M. Porez, V. Lebastard, A. J. Ijspeert, and F. Boyer, "Multi-physics model of an electric fish-like robot: Numerical aspects and application to obstacle avoidance," in *Proc. 2011 IEEE/RSJ Int. Conf. on Intelligent Robots and Systems,* (to appear in), (San Francisco, CA), 2011.

[17] S. Ferrari and R. F. Stengel, "Smooth function approximation using neural networks," *IEEE Trans. on Neural Networks*, vol. 16, no. 1, pp. 24–38, 2005.

[18] A. Crespi and A. Ijspeert, "Amphibot II: An amphibious snake robot that crawls and swims using a central pattern generator," in *Proc. 9th Int. Conf. on Climbing and Walking Robots*, (Brussels, Belgium), pp. 19–27, 2006.

[19] Y. Morel, M. Porez, A. Leonessa, and A. J. Ijspeert, "Nonlinear motion control of CPG-based movement with applications to a class of swimming robots," in *Proc. 50th IEEE Conf. Dec. Contr.*, (Orlando, FL), to appear in, 2011.

[20] ANGELS, "ANGuilliform robots with Electric Sense," *http://www.theangelsproject.eu*.